ELSEVIER

Biochimica et Biophysica Acta 1459 (2000) 148–168

BIOCHIMICA ET BIOPHYSICA ACTA
BBA

www.elsevier.com/locate/bba

Control of the photosynthetic electron transport by PQ diffusion microdomains in thylakoids of higher plants

Helmut Kirchhoff *, Sebastian Horstmann, Engelbert Weis

Institut für Botanik, Schloßgarten 3, D-48149 Münster, Germany

Received 27 January 2000; received in revised form 12 April 2000; accepted 13 April 2000

Abstract

We investigate the role of plastoquinone (PQ) diffusion in the control of the photosynthetic electron transport. A control analysis reveals an unexpected flux control of the whole chain electron transport by photosystem (PS) II. The contribution of PSII to the flux control of whole chain electron transport was high in stacked thylakoids (control coefficient, CJ(PSII) = 0.85), but decreased after destacking (CJ(PSII) = 0.25). From an 'electron storage' experiment, we conclude that in stacked thylakoids only about 50 to 60% of photoreducable PQ is involved in the light-saturated linear electron transport. No redox equilibration throughout the membrane between fixed redox groups at PSII and cytochrome (cyt) *bf* complexes, and the diffusable carrier PQ is achieved. The data support the PQ diffusion microdomain concept by Lavergne et al. [J. Lavergne, J.-P. Bouchaud, P. Joliot, Biochim. Biophys. Acta 1101 (1992) 13–22], but we come to different conclusions about size, structure and size distribution of domains. From an analysis of cyt b_6 reduction, as a function of PSII inhibition, we conclude that in stacked thylakoids about 70% of PSII is located in small domains, where only 1 to 2 PSII share a local pool of a few PQ molecules. Thirty percent of PSII is located in larger domains. No small domains were found in destacked thylakoids. We present a structural model assuming a hierarchy of specific, strong and weak interactions between PSII core, light harvesting complexes (LHC) II and cyt *bf*. Peripheral LHCII's may serve to connect PSII–LHCII supercomplexes to a flexible protein network, by which small closed lipid diffusion compartments are formed. Within each domain, PQ moves rapidly and shuttles electrons between PSII and cyt *bf* complexes in the close vicinity. At the same time, long range diffusion is slow. We conclude, that in high light, cyt *bf* complexes located in distant stromal lamellae (20 to 30%) are not involved in the linear electron transport.

Keywords: Microdomain; Plastoquinone; Photosystem II; Cytochrome *bf* complex; Thylakoid; Photosynthesis

1. Introduction

Chloroplast thylakoid membranes contain five integral protein complexes: (1) PSII core complex, most of which is associated with LHCII complexes, (2) a fraction of loosely bound LHCII (mobile LHCII), (3) the PSI core complex, associated with LHCI complexes, (4) the cyt *bf* complex which mediates electron flow between PSII and PSI and (5) the ATP-synthase complex (CFo–CF1). Of these com-

Abbreviations: cyt, cytochrome; DBMIB, 2,5-dibromo-3-methyl-6-isopropyl-p-benzoquinone; DCMU, 3-(3,4-dichlorophenyl)-1,1-dimethylurea; DMBQ, 2,5-dimethyl-p-benzoquinone; DQ, duroquinone; HEPES, N-2-hydroxyethylpiperazine-N′-2-ethane-sulfonic acid; LHC, light harvesting complex; MV, methylviologen; PQ, plastoquinone; PS, photosystem

* Corresponding author. Fax: +49-251-8323823;
E-mail: kirchhh@uni-muenster.de

0005-2728/00/$ – see front matter
PII: S0005-2728(00)00143-2

plexes, PSI–LHCI and PSII–LHCII and ATP-synthase have been demonstrated to partition in an unequal way between stacked grana membranes and destacked stroma lamellae. PSII–LHCII complexes and most of the mobile LHCII are located in the grana stacks, whereas PSI–LHCI and ATP-synthase are entirely excluded from stacked membranes [1–4]. Only a minor fraction of PSII, PSII β, has been found in the destacked, stroma-exposed regions of thylakoids. In contrast to the more or less strict compartmentation of these complexes, cyt *bf* complexes are distributed throughout all membrane regions, grana stacks, destacked grana regions (grana margins) and stroma lamellae [2,3]. The lateral flow of electrons throughout the membrane is thought to be managed by two mobile redox carriers which are strictly separated in two phases. Plastocyanin, a water soluble protein, migrates in the inner thylakoid space and mediates electron transfer between distinct docking sites at cyt *f* and PSI. The mobile pool of plastoquinone (PQ) (5 to 10 PQ per PSII) is associated with acyl lipids in the thylakoid lipid bilayer phase and binds to specific sites at PSII and cyt *bf* complexes.

The lateral separation of the two PS's, in conjunction with the unique localization of cyt *bf* throughout all membrane compartments raises the question of electron shuttling between PSII and cyt *bf* by PQ. Viewed from above, the grana discs are circular in shape with a diameter of 400 to 500 nm [5]. Assuming more or less random distribution of cyt *bf* complexes throughout the membrane, electron shuttling between all PSII and cyt *bf* requires the diffusion of PQ within a few ms (the turnover time of linear electron flow) over a distance of a few hundred nm. The oxidation of PQH_2 bound to the Q_o site at the cyt *bf* complex is assumed to be the slowest redox step in the electron transport chain and may limit light-saturated whole chain electron transport [6,7]. If PQ diffusion would be slow, PQH_2 oxidation and, hence, whole chain electron transport could be a diffusion limited process.

However, the situation is even more complex. As PQ is thought to diffuse very rapidly within a lipid bilayer phase, PQ seems to be an excellent candidate for long distance shuttling. In pure phosphatidylcholine vesicles a PQ diffusion coefficient of 1.3 to 3.5×10^{-7} cm^2 s^{-1} has been determined [8]. For PQ acting as a non-rate limiting carrier in electron flow throughout the membrane, the diffusion coefficient should be in the order of at least 2×10^{-8} cm^2 s^{-1} [9]. However, it has been argued, that the actual diffusion coefficient in thylakoids is reduced because PQ migration is restricted by closely packed transmembrane protein complexes. At least 50% of the membrane is occupied by transmembrane proteins [10,11]. As the lateral mobility of transmembrane proteins is considerably lower than that of small lipophilic molecules, such as quinones, protein density and distribution could be important factors determining the lateral migration of small molecules throughout the membrane [9,12,13]. The percolation theory (summarized in [14]) predicts a certain threshold (percolation threshold) where transmembrane proteins create a network of virtually immobile obstacles. Large aggregates formed by association between proteins are even more efficient diffusion barriers than randomly distributed single proteins. In a first approximation, the diffusion of small molecules in a membrane highly covered with transmembrane proteins can be described by the percolation theory for the diffusion of small tracers in an archipelago of obstacles [14,15]. The geometry of clusters formed by obstacles is influenced by the interaction energy between them which in turn determines the effectiveness to function as diffusion barriers for small tracers [16]. Low interaction energies give more ramified clusters where in turn high interaction energies induce more compact ones. In addition to the 'percolation' effect, where proteins are primarily regarded as obstacles in a diffusion space, the diffusion coefficient for small molecules in membranes may be further reduced by specific interactions between proteins and the lipid phase. The presence of proteins is expected to decrease the fluidity of the lipid phase [17].

Mitchell et al. [9] have determined whole chain redox kinetics in non-disturbed thylakoids and used the data to model PQ diffusion in thylakoids. Assuming PQ percolation between randomly distributed thylakoid proteins (with zero interaction energy), they came to the conclusion that, despite the high protein density, PQ diffusion throughout the membrane could still be fast enough to exclude diffusion-limitation of PQH_2 oxidation. Recently, however, Blackwell et al. [18] presented evidence, that the actual PQ diffusion coefficient determined in thylakoid

membranes (measured by pyrene fluorescence quenching technique) is in the range of 0.3 to 3×10^{-9} cm^2 s^{-1}, i.e. two orders of magnitude lower than values obtained in liposomes, and one order of magnitude lower than the minimal values calculated by Mitchell et al. [9] for non-diffusionally controlled PQH_2 oxidation. Blackwell et al. [18] came to the conclusion that (1) PQH_2 must be diffusion controlled and (2) slow PQ diffusion is not simply the result of protein density. They postulated protein–protein interactions creating virtually immobile protein boundaries, but could not specify these protein interactions.

Recently, Lavergne et al. and Joliot et al. [11,19–21] derived an elegant concept, which could solve the conflict 'diffusional' versus 'chemical' limitation of PQH_2 oxidation. From their striking observation, that no global redox equilibrium between the mobile PQ pool and 'fixed' redox components such as Q_A and cyt b_6 is achieved, they proposed the existence of small local PQ diffusion microdomains, bound by proteins and created by a flexible 2D network of proteins throughout the membrane. They regard this kind of microstructure as the result of a free random distribution of proteins. No specific association of membrane components is assumed. From the percolation theory, above a critical density, immobile or slowly moving transmembrane proteins are, indeed, expected to form flexible 2D networks of closed compartments preventing long range movement of small molecules. The occurrence of such compartments is predicted when at least 50% of the surface is covered by particles [15], a value which is close to that found for grana discs [11]. From their redox studies, Lavergne et al. [11] suggested an average thylakoid microdomain size, in which only a small number of PSII centers share a common local PQ pool of about 6 PQ per PSII. Mobile PQ molecules could be confined within these domains, on a short time scale. Within each domain, PQ diffuses rapidly. Simultaneously, due to crowding of transmembrane protein complexes, long-range migration of PQ throughout the membrane is severely restricted. Hence, only in the close vicinity of PSII (in grana stacks) has PQ easy access to cyt *bf* complexes. Provided all domains include at least one cyt *bf* complex, electron flow between PSII and cyt *bf* complexes could be a non-diffusion limited process, while long range PQ diffusion throughout the membrane is impeded.

Lavergne and Joliot [22] discussed, that this kind of microorganization could help to solve an inherent thermodynamic problem associated with diffusion-controlled electron transport processes. They bear the potential for dissipation of redox energy. The thermodynamic inefficiency could be minimized either by forming functional supercomplexes, thereby excluding any free diffusion of redox components, or by a microorganization which substantially reduces the diffusion distance between fixed redox components.

The microdomain concept could also be the structural basis for a functional compartmentation of thylakoids on a larger scale. Recently it is suggested that linear electron flow between PSII and PSI occurs in grana (from PSII in grana stacks to PSI in the grana margins) while cyclic flow is possibly located in the stroma lamellae [2,3,23,24]. PQ exchange between these compartments is assumed to be slow. About 20% of the thylakoid membrane is made up of stroma lamellae. There is a 14 to 18% excess of chlorophylls (Chl) associated with PSI and this fraction of Chl in association with the stromal fraction of cyt *bf* complexes could be attributed to the cyclic flow [3,24]. The 'excess Chl' possibly associated with the cyclic flow, would explain why about 10 quanta (instead of 8 quanta) are required per evolved O_2 (for a discussion see [24]). If one further remembers that PQH_2 oxidation at the cyt *bf* complex is the slowest redox step in linear flow and fast PQ diffusion is possibly restricted to microdomains in the close vicinity of PSII, one may predict that the light-saturated whole chain linear electron flow is only determined by the number of cyt *bf* complexes located in grana stacks. Hence, the microdomain concept could shed new light on the dynamic lateral organization of thylakoids.

In its present form, however, the microdomain concept is still preliminary. There is still uncertainty about the exact stoichiometric composition and stability of domains. Also, the model does not incorporate recent progress in the understanding of the molecular architecture of thylakoid complexes. In their model, Lavergne and Joliot [19,11] did not incorporate specific protein interaction and, for simplicity, assume circles as contours of protein com-

plexes. There is, however, an increasing understanding of the structure of thylakoid complexes and various kinds of specific associations formed between these complexes. PSII in grana stacks seems to occur as dimeric PSII–LHCII supercomplexes [25–27]. Three specific binding sites at PSII core complexes for 'strongly', 'medium' and 'loosely' bound LHCII have been identified [28]. The trimeric LHCII units themselves can aggregate to oligomeric complexes [29]. LHCII complexes are also essential for connecting membranes to grana stacks [30,31]. It is quite likely, that they contribute to create a more or less stable 2D network of associated complexes. LHC proteins are the most abundant proteins in thylakoids and may play an essential role not only in light harvesting but also in the ultrastructure and organization of thylakoids (see, for example, [32]).

In this study, we examine the role of PQ diffusion in the linear electron transport. A control analysis of linear electron flow and of cyt b_6 redox reveals an unexpected high flux control of the whole chain electron transport by PSII in stacked, but not in destacked thylakoids. In stacked membranes, only about 50 to 60% of PQ is involved in the light-saturated linear flux. The data support the microdomain concept of restricted long range PQ diffusion proposed by Lavergne and Joliot [19]. We extend their concept and come to different conclusions about the size, structure and distribution of domains. Lavergne and Joliot [19] and Lavergne et al. [11] propose a homogeneous and broad distribution of the stoichiometric composition of domains, with an average number of 3 to 5 PSII centers per domain, and domains are created by random distribution of proteins in a densely packed 2D percolation space. Specific structural interactions are not yet considered. From a control analysis of cyt *b* reduction in the presence of a different level of PSII activity we conclude a distinct heterogeneity in the microdomains organization. At least 70% of PSII may be located in small domains, with an average number of only 1 to 2 PSII centers (3 to 4 PQ per PSII) for each domain, while a small fraction of PSII is located in large domains (>10 PSII centers per domain). Another important feature of our model is the assumption that the domain borders are formed by a hierarchy of specific PSII–LHCII and LHCII–LHCII interactions. These interactions are assumed to create flexible strings and networks of associated proteins. We explain how moderate destacking at low Mg^{2+} concentration could disturb this organization, by disrupting specific interactions, without changing the protein density. We discuss a dynamic grana stack microorganization with respect to the control of the photosynthetic flux in higher plants.

2. Material and methods

2.1. Preparation of thylakoids

2.1.1. From spinach

Leaves from 6 to 8 week old plants grown in hypotonics at 13–16°C, 10 h light period (300 μmol quanta m^{-2} s^{-1}) were taken. Intact chloroplasts were isolated as in [33] and stored on ice. Before measurements, thylakoids were freshly prepared from chloroplasts by osmotic shock (30 s) in 7 mM $MgCl_2$, 80 mM KCl and 30 mM HEPES, pH 7.6 and stored in 7 mM $MgCl_2$, 80 mM KCl, 30 mM HEPES, pH 7.6 and 330 mM sorbitol ('stacked thylakoids'). 'Destacked thylakoids' were prepared in the same way except $MgCl_2$ was omitted and the concentration of KCl was 15 mM.

2.1.2. From tobacco

Leaves from 10 to 14 weeks old plants grown in a green house were homogenized in 50 mM KCl, 1 mM $MgCl_2$, 1 mM $MnCl_2$, 1 mM EDTA, 0.5 mM KH_2PO_4, 25 mM 2-(*N*-morpholino)-ethanesulfonic acid, pH 6.1, 330 mM sorbitol, 10 μM sodium ascorbate, 0.2% (w/w) bovine serum albumin and 2% polyvinylpyrrolidone. The homogenate was filtered and centrifuged (60 s, $2000\times g$). The pellet was separated from starch, resuspended and washed in 7 mM $MgCl_2$, 10 mM KCl, 50 mM HEPES, pH 7.6 and stored in a medium containing 7 mM $MgCl_2$, 10 mM KCl, 50 mM HEPES, pH 7.6 and 330 mM sorbitol. Thylakoids were prepared by osmotic shock (see Section 2.1.1) and stored and measured in a Mg^{2+}-containing (stacked) or Mg^{2+}-free (destacked) medium.

2.2. Electron transport

Electron transport was measured using a Clark type oxygen electrode (Hansatech) at 20°C in the

storage media (s.a.) in the presence of either 100 μM MV, 1 mM Na-acid and 1 μM nigericin (whole chain electron transport) or 1 mM DMBQ and 1 μM nigericin (PSII capacity) or 100 μM MV, 1 mM Na-acide, 1 mM DQ, 1 μM nigericin, 20 μM DCMU ('cyt *bf* capacity'). The duroquinone-dependent electron flux was corrected for an electron leak between duroquinone and plastocyanin, which was determined in the presence of 1 μM DBMIB. Excitation light was saturating for each condition (3000–7000 μmol quanta m^{-2} s^{-1}).

2.3. Chl a fluorescence

Chl *a* fluorescence was measured in a reflecting cuvette through a branched light guide. Green excitation light was filtered through glass filters (Schott BG 18 and Corning 9782) and a broad band passing filter (450–550) by Optical Coating Lab., Inc. (OCLI). Fluorescence was detected by a photomultiplier (EMI) protected by Schott AL 685 and heat reflecting filters. Before measurement, the oxygen concentration in the medium (10 μg Chl ml^{-1}, 1 μM nigericin, DCMU as indicated) was reduced by gently bubbling with nitrogen. Fluorescence induction was analyzed as in [34].

2.4. Cyt redox kinetics

Absorption transients were measured in a laboratory built single beam photometer. A weak measuring light from a monochromator (Bausch and Lomb) was focussed into a reflecting cuvette (1.75 cm optical path length) and detected by a photomultiplier (EMI), protected by broad band passing and heat reflecting filters (LOT heat reflecting filter, FD 245Q, OCLI green). 120 ms pulses of red excitation light (3000 to 4000 μmol quanta m^{-2} s^{-1}; Schott RG 630 cut off and heat protection filters) were directed through a light guide into the cuvette (90° position to the measuring beam). The storage medium contained 50 μM MV, 1 mM sodium-ascorbate, 1 μM nigericin, 1 μM valinomycin and thylakoids at a concentration equivalent to 18 μM Chl.

Repetitive pulse-induced absorbance transients were measured at four wavelengths: 548, 554, 563 and 575 nm. It was proven that the characteristic ΔpH-dependent light scattering changes and electrochromic changes peaking around 520 nm [35] were eliminated by the addition of nigericin and valinomycin. The contribution of other non-cyt signals was eliminated by a baseline correction of cyt spectra (difference between changes at 548 and 575 nm; see Fig. 1) similar to that described by Joliot and Joliot [36]. Small contributions of P700- and plastocyanin-dependent changes were calculated on the basis of published spectra (see under Table 1). The contribution of C550 was determined on the basis of a spectrum of this component derived as described below (see spectra in Fig. 1). After baseline correction and substraction of P700, plastocyanin and C550 contribution, cyt b_6- and f-dependent absorbance changes, Δabs, were calculated from the remaining changes at 554 and 563 nm as follows:

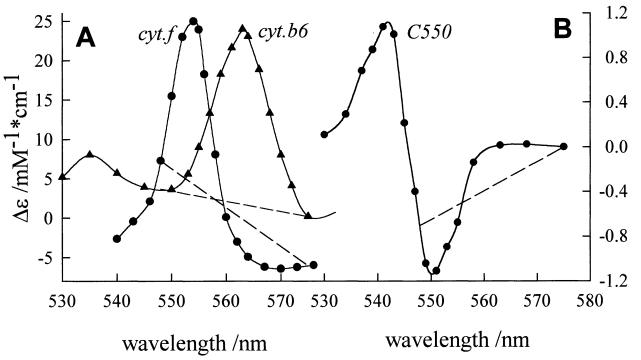

Fig. 1. Difference absorbance spectra of cyt *f*, cyt b_6 (A) and C550 (B). Spectra were obtained from light-induced absorbance changes in the following ways: cyt *f*: thylakoids were incubated in the presence of 50 μM MV, 1 μM nigericin, 1 μM valinomycin, 10 μM 2′,4′-dinitrophenylether of 2-jodo-4-nitro-thymol (DNP-INT), 5 μM 2,3,5,6-tetramethyl-*p*-phenylenediamine (DAD), 50 μM sodium ascorbate and illuminated with 500 ms far-red pulses (Schott RG 715). The spectrum was obtained from absorbance changes occurring between 400 and 1200 ms after the pulse. Cyt b_6: thylakoids were incubated at pH 8.0 in the presence of 50 μM MV, 1 μM nigericin, 1 μM valinomycin, 500 μM ferricyanide and illuminated with 500 ms light pulses (Schott RG 630 cut off and heat protection filters). The spectrum is obtained from absorbance changes occurring during 62 and 442 ms after the pulse. C550: PSII-enriched membranes (BBY particles) were incubated in the presence of 1 μM nigericin, 1 μM valinomycin, 10 μM DCMU and 2 mM ferricyanide and illuminated with 10 ms light pulses. The spectrum was obtained from the absorbance change during the first 10 ms after the pulse. All spectra were normalized to published absorbance coefficients (cyt *f*, [67]; cyt b_6, [68]; C550, [69]). Dashed lines indicate baselines derived from absorbance changes at 548 and 575 nm. Note the different scaling in (B).

$$\Delta\text{abs}(\text{cyt } b) = \frac{\Delta\text{abs}_{563}\cdot\Delta\varepsilon(\text{cyt } f)_{554} - \Delta\text{abs}_{554}\cdot\Delta\varepsilon(\text{cyt } f)_{563}}{\Delta\varepsilon(\text{cyt } f)_{554}\cdot\Delta\varepsilon(\text{cyt } b)_{563} - \Delta\varepsilon(\text{cyt } f)_{563}\cdot\Delta\varepsilon(\text{cyt } b)_{554}} \quad (1a)$$

$$\Delta\text{abs}(\text{cyt } f) = \frac{\Delta\text{abs}_{554}\cdot\Delta\varepsilon(\text{cyt } b)_{563} - \Delta\text{abs}_{563}\cdot\Delta\varepsilon(\text{cyt } b)_{554}}{\Delta\varepsilon(\text{cyt } f)_{554}\cdot\Delta\varepsilon(\text{cyt } b)_{563} - \Delta\varepsilon(\text{cyt } f)_{563}\cdot\Delta\varepsilon(\text{cyt } b)_{554}} \quad (1b)$$

Difference absorbance coefficients, $\Delta\varepsilon$, for cyt b_6 and f and for C550 were derived from light minus dark difference spectra obtained from absorbance changes induced by saturating light pulses under specific conditions (Fig. 1A and B).

2.5. P700 redox kinetics

The redox kinetics of the PSI reaction center Chl, P700, was measured following absorption signals at 705 nm using a photometer similar as described above, with the following modifications: (1) blue green excitation light (Schott BG18 and LOT heat reflecting filter); (2) to minimize contamination with a Chl *a* fluorescence, the multiplier (protected by a Balzers B40 interference filter) was placed 35 cm behind the cuvette. The remaining fluorescence signal was determined separately and subtracted; (3) the medium contained 6.3 μM Chl and Na-ascorbate was omitted and (4) a continuous far-red background light (Schott IL715 and LOT heat reflection) was present.

Single turnover flashes were given by a Xenon flash lamp (Walz; half width 8 μs). The exact position of the maximum of the P700 signal (705 nm) was determined by measuring a complete light pulse-induced difference absorption spectrum in the absence of far-red background light and in the presence of 50 μM 2,3,5,6-tetramethyl-*p*-phenylenediamine (DAD) and 5 mM Na-ascorbate (not shown).

3. Results

3.1. Characterization of destacked thylakoids

Thylakoid stacking is based on molecular interactions between LHCII–protein complexes [31] and controlled by a balance between hydrophobic interactions and repulsive ionic forces (see [30,31]). Surface charge screening by divalent cations such as Mg^{2+} is an important factor in stabilizing this balance [37]. In this study, we incubate thylakoids, previously isolated as stacked membranes, in either Mg^{2+}-free or Mg^{2+}-containing media to compare electron transport processes in destacked and in stacked membranes. In the following, thylakoids incubated in Mg^{2+}-free media are called 'destacked thylakoids'. We are aware that thylakoids treated in this way may not be Mg^{2+}-free in a strict sense. We expect some Mg^{2+} still to be bound to the membrane. By this treatment, membranes are less stacked but grana are still present, while complete swelling of thylakoids (formation of 'blebs') is achieved by more rigorous extraction of Mg^{2+} as, for example, by chelating agents [38]. We have chosen the moderate treatment to avoid the formation of blebs and to keep the membrane in a fully functioning state.

Destacking is usually reflected by a decrease in Chl *a* fluorescence yield. Complete destacking usually leads to a drastic decline in the variable part of fluorescence, F_v, and even a significant decrease in F_0, the fluorescence with open PSII centers [38]. The destacking treatment in this study caused only a

Table 1
Difference absorbance coefficients after baseline correction (see text)

Wavelength (nm)	$\Delta\varepsilon$ (cyt *f*)[a] (mM^{-1} cm^{-1})	$\Delta\varepsilon$ (cyt b_6)[a] (mM^{-1} cm^{-1})	$\Delta\varepsilon$ (P700)[b] (mM^{-1} cm^{-1})	$\Delta\varepsilon$ (plastocyanin)[c] (mM^{-1} cm^{-1})	$\Delta\varepsilon$ (C550)[a] (mM^{-1} cm^{-1})
554	20.5	4.3	0.5	0.0	−0.2
563	−4.2	22.5	0.9	0.0	0.3

[a]From the spectra shown in Fig. 1.
[b]From [70].
[c]From [71].

moderate decrease in F_v (about 60%; Table 2) while F_0 remained almost unaffected (not shown). Destacking is further reflected by an increase in transmittance, which is thought to reflect thylakoid swelling [39]. The low Mg^{2+}-treatment caused a light transmittance increase by about 30% (Table 2). This was a moderate increase. In the case of a complete destacking and bleb formation a more significant transmittance increase in the order of 150% would have been expected [39]. On the other hand, the decrease in 90° light scattering change peaking at 535 nm (15%; Table 2) seems to be more substantial. 20% changes were reported for 'bleb' formation [39]. These scattering changes have been related to changes in the intrinsic thylakoid membrane structure, rather than to swelling. We take Chl *a* fluorescence and transmittance changes as indication for a moderate reduction in the degree of stacking by which the grana structure is not entirely destroyed. On the other hand, destacking-induced scattering changes possibly reflect a substantial rearrangement of membrane complexes.

After destacking, the light-saturated linear electron transport ($H_2O \Rightarrow MV$) was first stimulated relative to that in stacked thylakoids (about 20%, 2 min after incubation in Mg^{2+}-free medium) and then declined slowly and even fell slightly below that in stacked thylakoids (Table 2). This secondary slow inhibition, also seen for the PSII-dependent ($H_2O \Rightarrow DMBQ$) and the cyt *bf*-dependent ($DQH_2 \Rightarrow MV$) electron flux (Table 2) seems to be a consequence of a general destabilization of thylakoid functions, often seen in Mg^{2+}-free preparations.

3.2. Control of linear electron transport

Table 3 shows coefficients for the flux control of whole chain electron transport ($H_2O \Rightarrow MV$) by the number of active PSII and cyt *bf* complexes, CJ(PSII) and CJ(*bf*). We derived the control coefficients following the control theory by Kascer and Burns [40] and define the coefficients as:

$$CJ(PSII) = d(et_{ss})/et_{ss}/d[PSII_{active}]/[PSII_{active}] \quad (2)$$

$$CJ(bf) = d(et_{ss})/et_{ss}/d[bf_{active}]/[bf_{active}] \quad (3)$$

$[PSII_{active}]$ and $[bf_{active}]$ stand for the fraction of active PSII centers and cyt *bf* complexes (after titrating these complexes down with inhibitors), et_{ss} for steady state electron transport ($H_2O \Rightarrow MV$). CJ values were derived from the initial slope of the relationship electron transport versus the fraction of active PSII (Fig. 2) and cyt *bf* (data not shown), respectively.

CJ(*bf*) was determined by measuring electron transport ($H_2O \Rightarrow MV$) at different levels of cyt *bf* activity. Cyt *bf* complexes were titrated down with the Q_o-site inhibitor DBMIB. For each DBMIB concentration, the activity of cyt *bf* was determined by the light-saturated electron transport in the presence of 1 mM DQH_2 (to keep the PQ pool reduced) and the PSII inhibitor DCMU (results not shown). In stacked thylakoids, the whole chain electron flux de-

Table 2
Electron transport and optical properties of thylakoids

		Destacked	Stacked	Ratio destacked/stacked
($H_2O \Rightarrow MV$)	spinach >15 min	468 ± 55 (4)	499 ± 62 (4)	0.93
	spinach >2 min	560 (1)	450 (1)	1.24
	tobacco >15 min	388 ± 8 (10)	326 ± 6 (10)	1.19
($H_2O \Rightarrow DMBQ$)	spinach	998 ± 54 (11)	1084 ± 52 (11)	0.92
	tobacco	1012 ± 103 (3)	1030 ± 111 (3)	0.98
(DQH2 ⇒ MV)	tobacco	341 (1)	379 (1)	0.90
F_v/F_0	spinach	2.76 ± 0.03 (3)	5.14 ± 0.31 (5)	0.54
Transmittance (548 to 575 nm)	spinach			1.28 ± 0.03 (5)
90° light scattering (535 nm)	spinach	85 a.u. (1)	100 a.u. (1)	0.85

Electron transport rates were measured with saturating light (>7000 μmol quanta m^{-2} s^{-1}) in the presence of 1 μM nigericin; 100 μM MV, 1 mM DMBQ, 1 mM DQH_2. The DQH_2-dependent electron transport rates were measured in the presence of 20 μM DCMU. 1 mM Na-acide was added when MV was used as acceptor. Electron leakage by a cyt *bf* 'bypass' was determined by measuring electron transport in the presence of 1 μM DBMIB. Electron transport is given in μmol electron pair mg Chl^{-1} h^{-1}. The number of measurements is indicated in brackets.

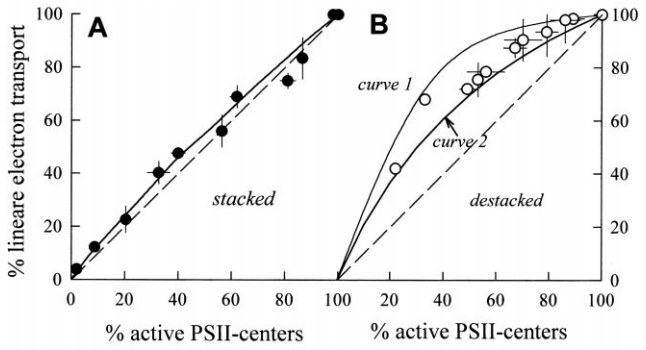

Fig. 2. Linear electron transport as a function of active PSII centers in stacked (A) and destacked (B) thylakoids. PSII-dependent ($H_2O \Rightarrow DMBQ$) and whole chain ($H_2O \Rightarrow MV$) electron transport was recorded from uncoupled (1 μM nigericin) spinach thylakoids in the presence of different aliquots of DCMU. The fraction of active PSII centers is calculated from PSII-dependent electron transport of inhibited, relative to non-inhibited, control samples. For both stacked and destacked thylakoids, 50% inhibition of PSII was achieved at about 50 nM DCMU. Note that DMBQ can only be reduced from active PSII, but not from 'non-QB-reducing' centers (see text). The solid curves in (B) are calculated using the model described in Fig. 3 and Appendix. Further details in the text.

creased almost linearly with the activity of cyt *bf* (fraction of active cyt *bf*) and the value for CJ(*bf*) was about 0.8 (Table 3). In destacked membranes, a somewhat lower CJ(*bf*) value of about 0.5 was derived. Relatively high values for CJ (*bf*) were expected, as PQH_2 oxidation at the Q_o site of cyt *bf* complexes is the slowest step in the electron transport chain and, hence, may significantly contribute to the flux control of the whole chain transport [6,7]. Values of 3.3 to 5 ms for the cyt *bf* turnover time were reported in the literature (for reviews see [41,42]). Electron transfer from cyt *f* to PSI (150 to 550 μs) is much faster and its contribution to the flux control should be much lower.

Fig. 2 shows the effect of different levels of PSII inactivation on the linear electron transport in stacked (A) and destacked (B) thylakoids. PSII activity was titrated down by the addition of small aliquots of DCMU. The fraction of PSII-centers inactivated by DCMU was calculated from the light-saturated PSII activity with DMBQ as an electron acceptor ($H_2O \Rightarrow DMBQ$) in an inhibited, relative to that in a non-inhibited, sample. DMBQ is reduced at the QB site of PSII and may not accept electrons from so called non-QB centers [43,44]. Virtually identical results were obtained when the fraction of active PSII-centers was derived from Chl *a* fluorescence induction curves (data not shown). In destacked thylakoids (Fig. 2B), the plot electron transport versus active PSII exhibits a curvilinear relationship and low values for CJ(PSII) (see Table 3). CJ(PSII) could vary between 0.20 and 0.35 for different preparations of destacked thylakoids. Relatively low control by PSII was expected as the overall turnover from H_2O to PQ is faster than the PQH_2 oxidation at the cyt *bf* complex: the transfer time from H_2O to PSII is in the order of 1 ms [45,46], the turnover time of PSII acceptor site reactions such as Q_B protonation [47], PQ exchange at the Q_A site [48] and transfer from PSII to cyt *bf* [9] are reported to be about 2 ms. Furthermore, the number of PSII exceeds that of cyt *bf* [49]. For our spinach thylakoids, we estimated about 2 PSII per cyt *bf* (not shown). Taking these numbers together, the capacity of PSII driven electron transport from H_2O to PQ may exceed that of the transfer from PQ to PSI by a factor of 3 to 5. Thus, assuming PQ to act as a diffusable redox carrier, the contribution of PSII to the overall flux control should be relatively low. The situation is described by a simple model of electron transport

Table 3
Control coefficients for PSII, CJ(PSII) and for cyt *bf*, CJ(*bf*) in stacked and destacked thylakoids

	Spinach destacked	Spinach stacked	Tobacco stacked
CJ(PSII)	0.25	0.83	0.67
CJ(*bf*)	0.51	0.88	

CJ(*bf*) is derived from two independent measurements.

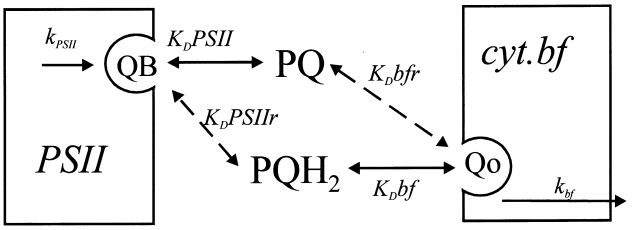

Fig. 3. Schematic presentation of an electron transport model used to calculate curves 1 and 2 in Fig. 2. Details of the model are described in Appendix. k_{PSII} and k_{bf} are overall rate constants of PSII and cyt *bf*-dependent electron transport. K_DPSII and K_DPSII$_r$ are dissociation constants for PQ and PQH_2 at the QB-binding site, K_Dbf and K_Dbf_r are dissociation constants for PQH_2 and PQ at the Q_o-binding site.

(Fig. 3) which includes PQ-binding at PSII and cyt *bf* and transfer processes on the basis of published rate constants. Furthermore, it is assumed that the 'ligand' PQ and PQH_2 can rapidly diffuse between all 'enzyme' binding sites within the reaction system (for further description see Appendix). Curves 1 and 2 in Fig. 2B are calculated from the model for slightly different sets of electron transport parameters (see Appendix). The area between the two curves fits the range of experimental data obtained with destacked thylakoids.

CJ(PSII) and CJ(*bf*) sum up in destacked thylakoids to a value somewhat lower than 1 (Table 3), indicating the contribution of other reactions (most likely diffusion and redox-turnover of PC) to the overall control. However, cyt *bf* complexes seem to dominate the control.

A different situation was found in stacked thylakoids. The plot was almost linear and CJ(PSII) values of 0.83 for spinach and 0.67 for tobacco were found (Table 3). Consequently, CJ(PSII) and CJ(*bf*) sum up to a value far above 1 (1.7 for spinach; Table 3). Obviously, the free PQ exchange concept does adequately describe electron transport in destacked, but not in stacked thylakoids. This is in clear conflict with the idea of free and fast PQ exchange between a large number of PSII and cyt *bf* complexes throughout the membrane. In contrast, there was a substantial discrepancy between the model and data points for stacked membranes (Fig. 2A).

3.3. Number of electrons stored in the PQ pool

Fig. 4 shows redox kinetics of P700 following a 120 ms saturated light pulse in the presence of far-red background light ($\lambda > 715$ nm). P700 is kept oxidized by the background light and then transiently reduced by the strong multiple turnover (120 ms) light pulse. Electrons for the reduction are deliberated at PSII and migrate to P700 via the PQ pool

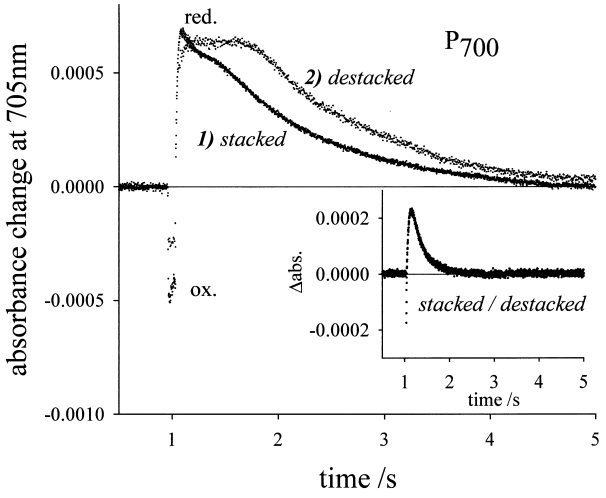

Fig. 4. Light pulse-induced P700 redox kinetics measured in stacked (curve 1) or destacked (curve 2) thylakoids. Tobacco thylakoids were illuminated with a far-red background light (16 W m^{-2}). Absorbance changes after a 120 ms saturating green (450–550 nm) light pulse were recorded (averaged from 30 repetitive signals, 0.09 Hz). The area below an absorbance transient induced by a single turnover flash was equal in stacked and destacked thylakoids. Further details in the text.

and cyt *bf* complexes. The area below the absorption transient is proportional to the number of electrons accumulated in the light and 'stored' in the PQ pool at the end of the pulse. This area was calibrated to that induced by a single turnover flash (equivalent to 1 electron per active PSII; see inset). The slow relaxation after the pulse (or flash) reflects the reoxidation of P700 by the relatively weak far-red background light. For the experiment shown in Fig. 4, we estimate 7.2 electrons for stacked (curve 1) and 10.8 electrons for destacked thylakoids (curve 2) in tobacco (Table 4). Independently, we calculated the total number of photoreducable PQ per PSII (PQ-pool size, expressed in electrons) from Chl *a* fluorescence induction during a 4 s illumination of anaerobic samples with relatively weak light. The maximum fluo-

Table 4
Electrons stored in PQ (for explanation see text)

	Tobacco destacked	Tobacco stacked	Spinach stacked
Electrons accumulating in PQ after a 120 ms pulse	10.8 (1)	7.2 ± 0.37 (4)	6.5 ± 0.6 (3)
'PQ pool size' (number of electrons)		11.8 ± 0.7 (3)	13.3 ± 1.3 (5)

Number in brackets indicate the number of independent measurements.

rescence was achieved after about 2s, a time assumed to be long enough to allow complete redox equilibration between 'fixed' and mobile redox components throughout the membrane. We derived about six photoreducable PQ (equivalent to 12 electrons) per PSII (Table 4). This is well within the limits of numbers reported by others [38]. The data in Table 4 indicate, that in destacked tobacco thylakoids, most photoreducable PQ is reduced during the 120 ms light pulse. It indicates, that redox equilibration is achieved throughout the membrane. In stacked membranes, however, only 7.2 electrons (6.5 for spinach) are stored during the light pulse, compared to a total pool size of 11.8 (13.3 for spinach). These numbers did not change significantly by varying the light pulse between 60 to 300 ms. The result indicates, that in tobacco about 40% of the PQ pool (50% in spinach) remains oxidized, i.e. has no rapid exchange with the QB site of PSII. Obviously, in stacked thylakoids no complete equilibrium throughout the membrane is achieved in saturating light.

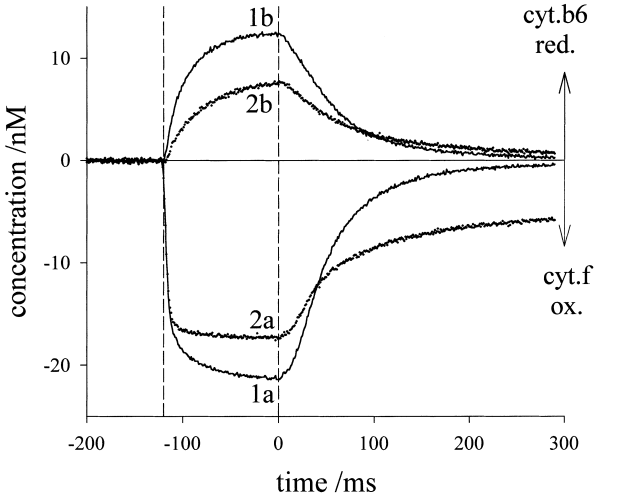

Fig. 5. Light pulse-induced cyt *f* and cyt b_6 redox kinetics in control thylakoids (curves 1a and 1b) and in thylakoids incubated in the presence of DCMU (curves 2a and 2b). Cyt redox kinetics were derived from 30 repetitive (0.09 Hz) measurements at 548, 554, 563 and 575 nm. Dashed lines indicate onset (left) and offset (right) of the pulse. Curves 1a and 1b, controls; curves 2a and 2b, 66% inhibition of PSII. Further details in the text.

3.4. Control of cyt b_6 photoreduction by PSII

Redox kinetics of cyt *f* and b_6 induced by 120 ms light pulses were analyzed. Photooxidation of cyt *f* is followed by the reduction of cyt b_6 (Fig. 5, curves 1a and 1b). This 'oxidant-induced reduction' of cyt b_6 is a first step in the Q-cycle pathway of electrons [41,42,50,51]. From a comparison of the light-induced cyt *f* signal with chemical difference spectra (data not shown) we conclude that virtually all cyt *f* is photooxidized under such conditions. Most cyt *f* was rapidly oxidized (half time about 3 ms), a small fraction of 15 to 20% slowly oxidized (half time about 25 ms). This 'slow' cyt *f* could be related to either an unknown side path for electrons or to a plastocyanin diffusion limitation. The slow component may not contribute to the fast linear electron flux.

At the end of the 120 ms light pulse, about 0.6 heme cyt *b* per cyt *f* was reduced. This is well in accordance with the observations of others [41,42,50,51]. The cyt *bf* complex contains two *b*-type hemes, b_6(LP) and b_6(HP). In the light, reduced cyt b_6(LP) may not significantly accumulate and, hence, may not contribute to the signal. Cyt *b* reduction requires PQH_2 bound to the Q_o site. Under reducing conditions, when there is enough PQH_2 to occupy all Q_o sites, the b_6 reduction level is at its maximum. If there is not enough PQH_2, less cyt b_6 will be reduced. Redox turnover at the Q_n site seems to have less influence on the cyt b_6 reduction level.

Table 5
Characterization of cyt *f* and cyt b_6 redox kinetics

	Destacked thylakoids	Stacked thylakoids	Ratio destacked/stacked thylakoids
Maximum cyt *f* oxidation[a]	1.13 ± 0.03	1.17 ± 0.02	0.97
Maximum cyt b_6 reduction[a]	0.61 ± 0.03	0.65 ± 0.02	0.94
$t_{1/2}$ cyt b_6 oxidation (ms)	47.5 ± 4.9	42.0 ± 5.1	1.13
$t_{1/2}$ cyt b_6 reduction[b] (ms)	14.1 ± 1.0	12.4 ± 0.9	1.14

[a]Values in mmol component mol^{-1} Chl.
[b]A lag time of 2 ms is subtracted. The results are from four independent measurements.

Thus, the cyt *b* reduction level may be taken as a relative measure for Q_o site occupation with PQH_2. In other words, the deficit in the cyt b_6 reduction level may reflect cyt *bf* complexes which do not have access to photoreduced PQ [21]. This interpretation is somewhat complicated by the fact that even under reducing conditions when all Q_o sites are occupied by PQH_2, some cyt b_6(HP) remains oxidized [50]. The explanation for this is still under debate. Nevertheless, it seems reasonable to take, in a first approximation, the maximum cyt b_6 reduction level experimentally obtained in a saturating multiple turnover pulse as a relative measure for Q_o sites occupied with PQH_2.

With active PSII (not inhibited by DCMU) the redox levels of cyt *f* and cyt b_6 were not significantly affected by destacking (Table 5). When PSII is titrated down by DCMU, the amplitude of the 'fast' cyt *f* remains constant, only the small slowly oxidizing component is inhibited (Fig. 5, 2a). In contrast, the cyt b_6 reduction level is reduced by DCMU (Fig. 5, 2b). We analyzed the time course of cyt b_6 reduction in inhibited, relative to that in non-inhibited, samples (Fig. 6). In moderately inhibited samples, a constant reduction ratio was achieved rapidly, while in highly inhibited samples ($>60\%$) it took up to 120 ms to achieve the maximum. Fig. 7 shows the relationship between the reduction ratio achieved after 120 ms versus PSII activity. In destacked thylakoids, the relationship was curvilinear. Up to 50% PSII inhibition cyt b_6 reduction was little affected, indicating that a relatively small number of PSII is able to provide all cyt *bf* complexes with electrons, via the PQ pool. In stacked membranes, the coupling between PSII activity and cyt b_6 reduction is much stronger. Over a wide range, the relationship is linear, but does not extrapolate to the zero point. The data points could be fitted by a complex function which will be discussed later.

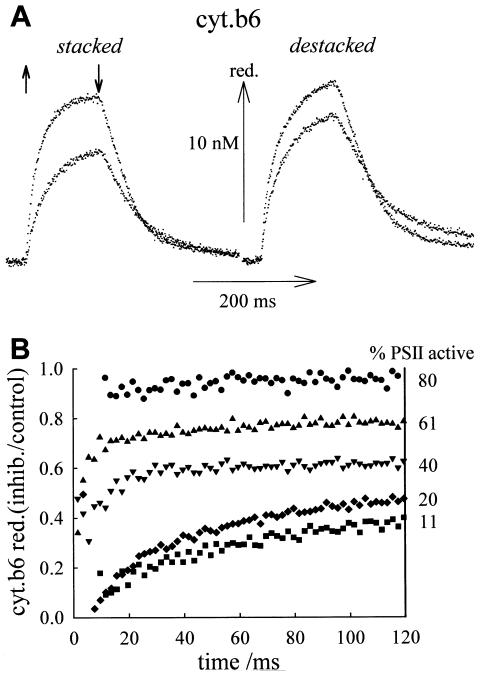

Fig. 6. The influence of PSII inhibition on cyt b_6 reduction. (A) Cyt b_6 redox kinetics for stacked and destacked spinach thylakoids. Conditions as for Fig. 5. Addition of a small aliquot of DCMU (66% PSII inhibition) causes a decrease in cyt b_6 reduction. Note the different cyt b_6 inhibition in stacked and destacked thylakoids. The light pulse is indicated by an upward (on) and downward (off) arrow. (B) Time course of the cyt b_6 reduction in inhibited, relative to non-inhibited stacked thylakoids. The curves are derived from cyt b_6 kinetics (as in A) in the presence of DCMU, divided by redox transients in the absence of DCMU. The numbers on the right side indicate the PSII activity adjusted by DCMU.

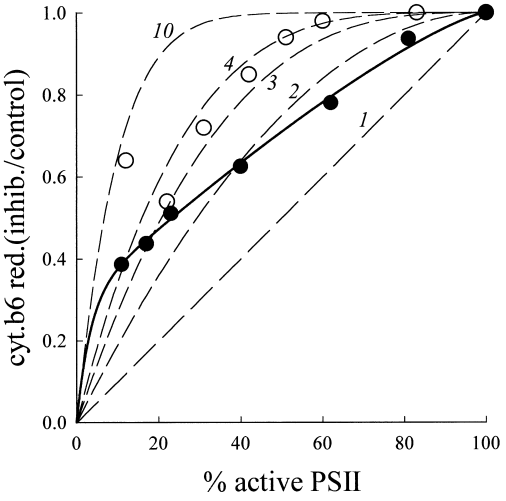

Fig. 7. Cyt b_6 reduction as a function of active PSII in stacked (closed circles) and destacked (open circles) thylakoids. For each level of PSII activity, the cyt b_6 reduction after 120 ms illumination, relative to that of a non-inhibited sample (see curves in Fig. 6B) were taken. Dashed curves are calculated from Eq. 6, where numbers indicate *n*, the number of PSII sharing a common PQ pool. The solid line represents a two component function from Eq. 6, with $n=1.3$ (70%) and $n>10$ (30%). Further explanations in the text.

3.5. Quantum yield of PQ photoreduction

Photoreduction of the PQ pool was followed by Chl *a* fluorescence induction in the absence of DCMU. The inset in Fig. 8A shows the variable part of fluorescence induction (F_v, fluorescence increase from F_0 to F_m level), measured at different actinic light intensities. The maximal levels of F_v from the different curves were set to one. The time required to complete induction decreases with actinic light intensity (curve 1 to 4). Reoxidation of PQ by cyt *bf* complexes was minimized by low temperature (7°C) and anaerobiosis (gentle N_2-bubbling). Over the range of light intensities used, the total area above fluorescence induction correlated linearly with the intensity, suggesting that there was no significant 'electron leakage' which would have affected the fluorescence induction. A fast initial increase in the fluorescence curve (Fig. 8A, inset) reflects PSII centers which do not equilibrate with the PQ pool

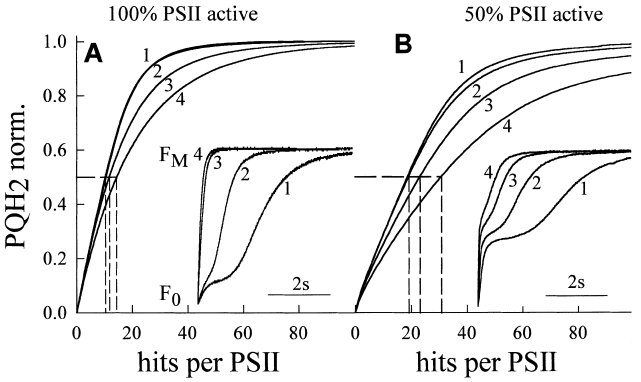

Fig. 8. PQ photoreduction as a function of the number of hits per PSII at different light intensities for control (A) and thylakoids in the presence of DCMU (B). Stacked thylakoids were preincubated for 15 min at 7°C in the presence of 1 μM nigericin in the dark. Under such conditions, reoxidation of PQH_2 is minimized. Chl *a* fluorescence was recorded at different light intensities. The variable part of fluorescence was normalized. PQ photoreduction was calculated from the growth of the area above the fluorescence curve and recorded as a function of accumulated hits per PSII (time axis multiplied with the rate of hits per PSII). The rate of hits per PSII was calculated for each light intensity from fluorescence induction in the presence of saturating DCMU (20 μM) as in [34]. The intensity of excitation light (450–550 nm) was: curve 1, 22 μmol quanta m^{-2} s^{-1}; curve 2, 46 μmol; curve 3, 90 μmol and curve 4, 151 μmol. (A) Control; (B) 50% PSII inhibition. For each PQ reduction curve, the dashed line indicates the 50% reduction point.

(possibly so called 'non-QB centers'; (see [38]). PQ photoreduction was calculated from the growth of the area above fluorescence. To compare the quantum efficiency of PQ photoreduction at different actinic light, PQ reduction was plotted against the number of photoreactions ('hits') per PSII (Fig. 8A). The number of hits per PSII was derived from a comparison with fluorescence induction in the presence of saturating DCMU (20 μM), following a procedure described by Trissel and Lavergne [34]. The slope of these curves reflects the quantum yield of the PQ reduction, defined as the number of quanta (hits) required to reduce PQ. In low actinic light the PQ photoreduction curves are almost linear over a wide range (curves 1 and 2). Ten hits were required to reduce 50% of the PQ pool. The total number of photoreducable PQ was calculated to be about seven (equivalent to 13.8 electrons) per PSII (from the area above fluorescence induction in the absence of DCMU, compared to that in the presence of DCMU, see [52]). At higher actinic light the PQ photoreduction curves were less linear and the quantum requirement for 50% PQ reduction increases (e.g. about 28 electrons at 120 μmol quanta m^{-2} s^{-1}; curve 4). Fifty percent inhibition of PSII by DCMU caused an initial fast increase in the fluorescence induction (reflecting blocked centers; Fig. 8B, inset) and an overall decrease in the quantum yield of PQ reduction. With 50% active PSII in low light, about 19 hits are required to reduce 50% PQ (Fig. 8B). However, the *relative* decrease in the quantum yield with increasing actinic light (>50 μmol quanta m^{-2} s^{-1}) was similar to that seen in samples without DCMU (Fig. 8B, curves 1 to 4).

In principle, it would be interesting to obtain similar information from destacked membranes. However, we did not carry out such experiments. Due to LHCII detachment and energy spillover from PSII to PSI [38], the variable part of fluorescence in destacked membranes is highly quenched (see Table 2) and fluorescence signals could be difficult to interpret.

The normalized quantum yields derived from these experiments (defined as hits required for 50% reduction of PQ) were plotted against the time interval (dark intervals) between hits per PSII (Fig. 9). In low light (dark interval >60 ms) the quantum yield was at its maximum. Under such conditions, we as-

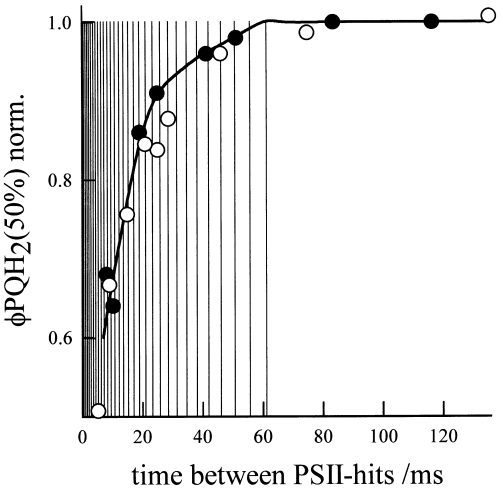

Fig. 9. The quantum efficiency of PQ photoreduction as a function of dark intervals between photocycles at PSII. The quantum efficiency, Φ, is defined as the reciprocal of hits per PSII required for 50% reduction (see Fig. 8). The values for Φ were normalized to the highest value. Other conditions as for Fig. 8. Closed circles: control, open circles: 50% active PSII.

sume redox equilibration between each PSII and a large amount of PQ to occur in the dark periods between single photoreactions. Above a certain threshold (dark intervals < 60 ms) the quantum requirement for PQ reduction increases with light. Since the redox potential, E_m, of diffusable PQ/PQH_2 is at least 100 mV more positive then that of the fixed redox couple, Q_A/Q_A^- [48], accumulation of Q_A^- is only expected if virtually all diffusable PQ is reduced in the vicinity of PSII centers. Thus, the result points to a disequilibration of PQ and PQH_2 throughout the membrane in high light. Obviously, 'closed' PSII centers (with Q_A^-) do accumulate while a large fraction of the diffusable PQ is still oxidized. The time of 60 ms may reflect the minimum time required to achieve redox equilibrium between Q_A and the PQ pool.

4. Discussion

4.1. No free diffusion of PQ

The electron transport through the cyt *bf* complex (turnover time 3.3 to 5 ms; see [41,42]) is the slowest step in the electron transport chain [7]. The reaction is probably limited by internal transfer reactions within the high potential chain (Rieske center and cyt *f*; see, for example, [21]). Downstream transfer to PSI via the mobile carrier plastocyanin is much faster (150 to 550 μs [7]). Turnover times of the transfer from H_2O to PSII centers [45,46] and from Q_A to diffusible PQ [47,48] are in the order of 1 and 2 ms, respectively. Considering the turnover rates and the number of PSII centers, relative to that of cyt *bf*, the capacity of electron transfer from H_2O to PQ is expected to exceed that of the cyt *bf* mediated transfer by a factor of 3 to 5. If one further regards PQ as a rapidly diffusing carrier, the contribution of PSII to the control of whole chain electron flux should be low.

For destacked membranes the predictions for the electron transport between PSII and cyt *bf* with PQ as a diffusible carrier are nearly fulfilled. CJ(PSII) is much lower than CJ(*bf*) and the two coefficients sum up to values around 0.8 (Table 3). According to the control theory [40,53], the sum of all individual control coefficients in a linear sequence of enzyme reactions should not exceed one, provided all substrates can migrate and interact with a large number of enzymes. It suggests that the electron transport chain in destacked thylakoids is mainly controlled by cyt *bf*. For stacked thylakoids, however, the situation is different. The whole chain electron flux decreases almost linearly with the number of active PSII (Fig. 2A) and the value for CJ(PSII) is about as high as that for CJ(*bf*) (Table 3). Both control coefficients sum up to a value not far below 2. This is in clear contradiction to the concept of PQ as a rapidly diffusing long range carrier between randomly distributed PSII and cyt *bf* complexes. Rather, it points to restricted diffusion between a limited number of PSII and cyt *bf* complexes.

Another argument against PQ as a rapidly diffusing carrier comes from the cyt *b* redox kinetics. In a free exchange system, the capacity of about 50% active PSII should be sufficient to provide most cyt *bf* complexes with electrons, as is actually seen in destacked thylakoids (Fig. 7). In stacked thylakoids, there is a much closer correlation between PSII activity and cyt *b* reduction. This can be explained by the assumption, made by Joliot et al. [11,21], that rapid electron shuttling by PQ/PQH_2 is restricted to small diffusion areas in the close vicinity of PSII centers. The results indicate that by titrating down

the number of active PSII, an increasing number of cyt *bf* complexes seems to have no access to photoreduced PQH_2.

Our results and observations made by Lavergne et al. [11] support the conclusion that due to the inability of PQ to migrate rapidly throughout the membrane, no global redox equilibrium between the 'fixed' redox component, Q_A, and the diffusible carrier PQ is achieved. During a 120 ms pulse, about 60 photocycles are expected to occur at each PSII center (assuming a PSII turnover time of 2 ms) and nearly all Q_A accumulates in its reduced form (from Chl *a* fluorescence, not shown). This is by far enough to photoreduce virtually all free PQ molecules in the thylakoid membrane (about six PQ/12 electrons per PSII center; see above), provided PQ moves rapidly throughout the membrane. In destacked thylakoids, nearly all PQ becomes reduced by the pulse (11 electrons 'stored' in the electron transport chain, equivalent to 5–6 PQH_2; see Table 4). In stacked membranes, however, a large fraction of PQ remains oxidized (about 40% in tobacco and 50% in spinach thylakoids; Table 4).

4.2. Microdomains

To explain these observations we adopt and further develop the microdomain organization concept proposed by Lavergne et al. [11,19]. In this concept, a microstructure is assumed, in which rapid PQ diffusion is restricted to small lipid microdomains in the vicinity of active PSII and surrounded by transmembrane protein complexes. Within each domain, PQ moves rapidly and only a few PSII and cyt *bf* complexes share a small PQ-pool. Long distance PQ migration is slow, as it requires crossing many domain boundaries. This microorganization allows rapid short distance electron shuttling between PSII and cyt *bf* in a close vicinity while, at the same time, redox equilibration throughout the membrane is slow. This would solve the apparent discrepancy between the observed slow PQ diffusion [18] and the suggestion of PQH_2 oxidation at the Q_o site as a non-diffusion limited process [9].

Our electron storage experiment reveals, that in stacked thylakoids 3–4 PQ (equivalent to 6–8 electrons) per PSII center became photoreduced in saturating light. Provided all active PSII is located in PQ diffusion domains (which is a reasonable but not a necessary assumption) each domain may contain an average of 3 to 4 PQ per PSII. Information about the actual number of active PSII centers per domain can be drawn from the DCMU titration data of cyt b_6 photoreduction in the following way: gradual inhibition of PSII should lead to the existence of 'active' and 'inactive' domains. Inactive domains (with all PSII centers blocked and all PQ in the oxidized state) could be identified by the 'deficit' of the cyt *b* reduction level (see experiment in Fig. 7). The occurrence of domains, $P(x)$, containing n (PSII) centers can be estimated from the macroscopic relative number of active centers x $(0 > x > 1)$ with a binomial distribution, where k is the fraction of centers blocked by DCMU:

$$P(x) = \frac{n!}{(n-k)!k!} x^{(n-k)} (1-x)^k \quad (4)$$

The probability of microdomains where all centers are inactive (PSII blocked by DCMU; $k = n$) is then given by:

$$P(x) = (1-x)^n \quad (5)$$

As we identify those domains from the fraction of cyt b_6 not reduced in a light pulse, Eq. 5 can be written as:

$$(1-\text{cyt } b_{red}) = (1-x)^n \quad (6)$$

In Fig. 7 cyt b_6 reduction in inhibited, relative to that in non-inhibited, thylakoids was plotted as a function of active PSII centers. The photoreduction of cyt b_6 is a relatively slow process ($t_{0.5}$ is about 15 ms, see Fig. 6), limited by internal transfer processes rather than by PQH_2 binding (e.g. in [21]). Accumulation of photoreduced PQ and occupation of the Q_o site at cyt *bf* complexes should be completed much faster. Assuming about 2 ms PSII turnover time most PQ molecules and cyt b_6 should be reduced during the 120 ms light pulse, provided they share a common rapid diffusion space with active PSII ('active domains'). At the same time, Q_o sites in domains with no active PSII centers ('inactive domains') remain unoccupied, as reflected by a deficit of cyt b_6 reduction. Thus, for each sample the relative cyt b_6 reduction level will give us the fraction of active domains (with at least one active PSII). Furthermore, the curvature of the function cyt *b* reduc-

tion versus active PSII centers reflects the average number of PSII per domain, *n* (see dashed curves in Fig. 7). The curvature increases with *n*. *n* should not be taken as a fixed stoichiometric number. The calculated curves represent functions expected for a *homogeneous* random distribution of all PSII among domains of different size, with *n* as the average number (see curves in Fig. 7). For destacked thylakoids, data points fit a curve for $n=4$ reasonably well. It should be noted, however, that with increasing *n*, data fitting becomes less reliable (see Fig. 7). However, whatever the exact number might be, the data suggest that in destacked thylakoids several PSII centers share a common PQ pool and the domain size distribution is homogeneous. In stacked membranes, the data clearly do not fit a function describing a homogeneous distribution. The solid curve in Fig. 7 seems to fit the data reasonably well. It represents a two-component function, describing a distribution of PSII between a large fraction (70%) located in very small domains (average number $n=1.3$, i.e. 1 or 2 centers per domain) and a small fraction (30%) located in large domains ($n>10$).

Lavergne et al. [11,19], using stacked membranes, arrived at the conclusion that the average number of PSII per domain is 3 to 4, with a homogeneous distribution in the domain size. Yet, there was no direct proof for the *homogeneity* in the distribution of the stoichiometric composition of domains. They derived the domain size from PQ reduction, relative to the PSII activity. They found a deficit in PQ reduction by about 60% with respect to the control, where about 85% of PSII was inhibited by DCMU. From this single titration step, they derived an average number of 3 to 4 for *n*. The rational behind our own analysis is quite similar. We compare PSII activity and cyt *b* reduction, which, in turn, reflects the accessibility to photoreduced PQ. When we assume homogeneity and calculate *n* for about 85% PSII inhibition (15% active PSII, see data for stacked thylakoids in Fig. 7), we also arrive at a number of 3 to 4 for *n*. Insofar, no discrepancy between their and our data exists. However, our analysis covers a much wider range of PSII inhibition. The complete titration clearly suggests a *non*-homogeneous distribution with one large pool of very small domains in stacked thylakoids.

As the plot cyt *b* reduction versus PSII (Fig. 7) seems to extrapolate to zero, we may assume that all domains do contain at least one cyt *bf* complex. If this is a correct assumption, it could have an interesting consequence with respect to the structure of domains. Random distribution and arrangement of proteins (percolation model) should result in a certain fraction of cyt *bf* free domains [11]. If no such 'empty' domains exist, it is likely that domains exhibit a more *specific* organization, possibly by specific protein–protein interactions.

4.3. Structure of microdomains

We developed a hypothetical structural model for microdomains in grana stacks (see Fig. 10), which is based on conclusions drawn from the analysis in this study and on the current knowledge about the molecular architecture of PSII, LHCII and cyt *bf* complexes. Usually, the largest fraction of LHCII is localized in grana stacks. It should be regarded as an important complex not only for light harvesting but also for the ultrastructure of grana, e.g. [32]. LHCII proteins (Lhcb1–6) are the most abundant proteins in grana and are important factors in grana stacking. Three of these LHCII proteins (the gene products Lhcb1, Lhcb2 and Lhcb3) form a trimer with a highly resolved structure [54], the remainder of these proteins are monomeric. Some of the trimeric LHCII's bind to CP 43 and CP 47 with the monomeric LHC proteins in-between [27]. PSII cores are assembled to antiparallel dimers [25,27]. Three specific binding sites at the PSII core complex for strongly, medium and loosely bound LHCII trimers have been identified [28]. Multiple forms of PSII–LHCII supercomplexes, containing two antiparallel PSII cores and at least 2 LHCII trimers (1 trimer per PSII center) have been isolated. The actual number of LHCII trimers per PSII in situ is in the range of 3 to 4. This exceeds the number of LHCII found in isolated complexes and is in good agreement with the suggestion that in addition to directly attached trimers there exists a pool of 'peripheral' LHCII complexes [55]. This peripheral pool has possibly a function not only in light collection but also in energy distribution and exchange between PS's. Peripheral LHCII may connect single LHCII–PSII supercomplexes to larger assemblies, mainly by LHCII–LHCII interactions. Different to the relatively strong

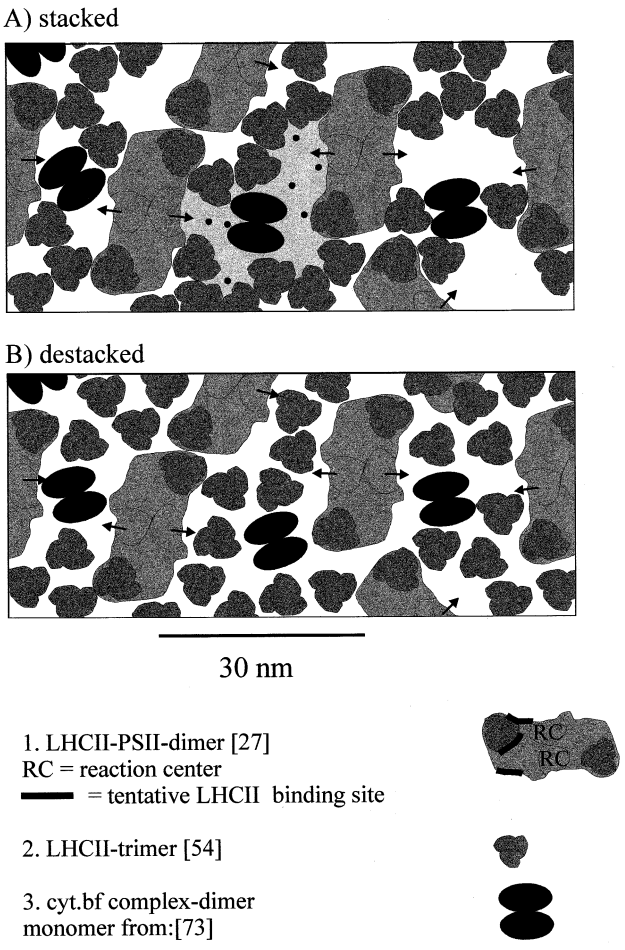

Fig. 10. Tentative assembly of membrane complexes in stacked (A) or destacked (B) grana membranes (top view). (A) The shaded area represents one selected example of a PQ diffusion domain containing two PSII centers. Small dots represent PQ rings, arrows indicate PQH_2 releasing sites (QB) for each PSII center. Tentative LHCII binding sites at PSII core complexes are marked by solid lines (see PSII–LHCII supercomplexes, lower part of the figure). Note the assembly between a large number of PSII–LHCII supercomplexes, mediated by weak LHCII–LHCII interactions. (B) It is assumed that electrostatic repulsive forces overcompensate attractive Van der Waals forces between LHCII's (due to low Mg^{2+}). Relatively stable dimeric PSII–LHCII supercomplexes (2 PSII, 2 LHCII) are still present, but are detached from each other. Note the free diffusion path between supercomplexes. Further details in the text.

associations within the PSII–LHCII supercomplexes, the 'peripheral' interactions between supercomplexes could be weak. However, even if these interactions are weak, they should exist: in well stacked membranes, several PSII centers share a common antenna system and excitation energy is exchanged between PSII centers (see [56]). This exchange is mediated by LHCII pigments [57] and requires a structural attachment between PSII–LHCII supercomplexes.

Peripheral LHCII can be phosphorylated (see [31,58]). In the phosphorylated state they are detached from PSII and then tend to migrate out of the grana into destacked regions. As a consequence, the PSII-absorption cross section and the degree of connectivity between PSII centers in the grana decreases. The migration of phosphorylated LHCII's is accompanied by a shift of one fraction of cyt *bf* complexes from stacked to destacked regions [59]. Obviously, peripheral LHCII's play an essential role not only in the assembly of PSII–LHCII supercomplex associations, but also in the compartmentation of cyt *bf* complexes.

From [20] and results in this paper, the conclusion is drawn that the diffusion path of PQH_2 is restricted to small domains where it attempts to find a cyt *bf* complex in the close vicinity of PSII centers. We further assume that about 50% of the membrane is occupied by integral proteins (see discussion in [11]). Associations between PSII–LHCII supercomplexes, as discussed above, lead to closed lipid membrane compartments bound by a PSII–LHCII network as illustrated in Fig. 10A. Cyt *bf* complexes probably occur structurally as dimers (see discussion in [50]). In this form, they exhibit a size comparable to that of LHCII trimers and can be integrated into a PSII–LHCII network. As there is no information about the interaction between cyt *bf* and LHCII we assume zero interaction energies.

Each of these compartments contains an average of four PQ molecules per PSII (see above) and should be seen as a PQ/PQH_2 diffusion domain. As PSII cores are associated in an antiparallel mode, the QB site of each center belongs to a different domain.

As the peripheral interactions between PSII–LHCII supercomplexes are weak, the domains should be seen as dynamic structures. They rearrange continuously, but are quasi stable with regard to the fast electron transport. Electrons are shuttled within a few ms between PSII and cyt *bf*. The 60 ms threshold for the maximum quantum yield for PQ photoreduction could reflect, in a first approximation, the average turnover time for rearranging domains. Several electron transport cycles could occur in high light during the average lifetime of a domain. Inter-

estingly, assuming zero interaction energies between thylakoid protein complexes and a circular shape of these complexes, Drepper et al. [60] concluded from Monte Carlo simulations that the average lifetime of PQ diffusion domains is only about 10 ms. Thus, domains may not be stable enough to efficiently restrict long range migration of PQ. Obviously specific interactions between complexes are crucial factors in stabilizing domains.

A decrease in the Mg^{2+}-concentration leads to a general increase of the electrostatic repulsive forces between charged integral thylakoid complexes. It causes detachment of stacked membranes (stacking is mediated by LHCII proteins) and lateral separation of PSII–LHCII supercomplexes. The overall protein density remains unchanged. In this state, despite a high protein density, the rapidly moving PQ molecules could worm their way between complexes and move rapidly throughout the membrane (Fig. 10B).

The model is still hypothetical. It explains the control of electron transport and still includes important features of the original microdomain concept by Joliot and Lavergne [11]. However, different to their concept, we propose that domains are formed by a hierarchy of *specific* protein interactions, rather than by randomly distributed proteins in a percolation space. It raises a number of questions, in particular concerning the assembly of such a complex structure. Possibly, phosphorylation/dephosphorylation of Lhcb4 and Lhcb5 subunits play an important role in controlling the assembly of this microdomain structure.

4.4. Microdomains and electron transport

Small domains consisting of only one or two PSII centers per domain seem to come close to the structure of PSII–cyt *bf* electron transport supercomplexes. Electron transport supercomplexes have been proposed for bacterial systems [61]. However, microdomains differ from such supercomplexes in many respects. Firstly, supercomplexes exhibit a fixed stoichiometric composition, while flexibility in its stoichiometric composition is an important feature of the domain concept. It allows dynamic adjustments of the stoichiometric composition of thylakoid complexes, an important factor in the acclimatization of photosynthesis to environmental and metabolic conditions [62].

Secondly, supercomplexes may be regarded as relatively stable structures, by which reactions in sequence are catalyzed step by step, without a lateral exchange of intermediates between single complexes. This may be an optimal structure for bacterial systems, in which the electron transport is driven by one photoreaction. In plant photosynthesis, optimal electron transport requires a subtle adjustment of the rate of two photoreactions. As discussed above PQ diffusion domains are not entirely stable. Slow lateral diffusion of PQ/PQH_2 is possible. This may help to avoid transient closure of centers at low light and, hence, to keep the quantum yield high. The domain structure would be of relevance for the electron transport at high electron fluxes only (with high frequency of photocycles). Due to the dynamic structure of domains, a progressive lateral redox imbalance will develop with increasing light throughout the membrane: at high light PQH_2 will accumulate in grana stacks, while in stroma lamellae, PQ is kept oxidized, even in high light. Hence, in high light, fast electron transport is restricted to grana, while cyt *bf* complexes located in stroma lamellae do not contribute to the linear flux. Stacking and compartmentation of cyt *bf* complexes could then be important factors in controlling the maximal rate of the linear electron flux. This kind of structural flux control is demonstrated by the destacking-induced stimulation of electron transport.

Another consequence of restricted PQ mobility is a compartmentation of the linear electron transport on a larger scale. Since active PSII is concentrated in grana stacks (see [24]), only the fraction of cyt *bf* complexes located in stacks can be involved in the linear flux. In our thylakoid preparations, about 75% of total cyt *f* was associated with grana (from fractionation experiments; not shown), which is in good agreement with the data from others, e.g. [59]. Such strict compartmentation is not expected for destacked thylakoids. These suggestions are in accordance with the observations that (1) a substantial fraction of PQ remains oxidized during a saturating light pulse in stacked, but not in destacked membranes (electron storage experiments; see Table 4) and (2) the steady state electron flux is stimulated by about 20% upon destacking (Table 2). Probably, the stim-

ulation is even somewhat underestimated, as it is followed by a slight inhibition of electron transport, possibly due to a general destabilization of membrane complexes by the low salt treatment. This is probably also the reason why no destacking-induced stimulation in the cyt *b* reduction level was seen. Repetitive spectroscopic determination of redox kinetics were carried out 5 to 20 min after destacking, i.e. after the inhibition of electron transport has taken place.

4.5. Plastocyanin diffusion

There is a large number of thermodynamic arguments why redox transfer by soluble carriers is less efficient than transfer between carriers which are strictly positioned in a membrane [22]. However, during the evolution of the oxygenic photosynthesis of plants, the spatial separation of the two PS's became a necessity to avoid wasteful shortcut of excitation energy between them (for a discussion see [63]). Thylakoid stacking is the structural basis for separation. This, however, bears the requirement for long distance electron shuttling. Due to microdomain formation within the lipid bilayer, long distance migration by PQ is restricted and the burden of long range shuttling is shifted to plastocyanin in the lumenal space. Plastocyanin is a spherical hydrophilic 10 kDa protein which carries its redox group, a copper atom ligated to 2 histidine, 1 cysteine and 1 methionine, well-protected within the protein matrix [64]. Fast electron transfer (lower μs range) proceeds as intramolecular transfer after tight binding to specific docking sites at either cyt *f* or PSI. Thus, dissipative and short circuit reactions during long range electron transfer should be minimal. Different to plastocyanin, PQ is a small and relatively reactive molecule which could undergo short circuit or even harmful side reaction.

Actually, a shift in the plastocyanin concentration between grana and stroma lamellae during light-dark transition was interpreted as favoring the long distance transport between these compartments [65]. However, there are conceptual difficulties with plastocyanin diffusion too. The lumenal space is narrow, with a number of proteins protruding into the lumen, and it is not yet entirely clear whether plastocyanin can diffuse rapidly enough over the whole distance of a few hundred nm between grana stacks and stroma lamellae (for discussion see, for example, [50]). Delosme [66] arrived at the conclusion that slow cyt *f* oxidation can be diffusion limited and has interpreted differing cyt *f* oxidation rates to correspond to different plastocyanin diffusion distances. The lag phase in the P700 oxidation after the saturating pulse (experiment in Fig. 4) seen in *destacked* membranes points to a rapid thermodynamic equilibration throughout the membrane between PQ and P700 mediated by PC (discussed in [74]). Interestingly, this lag phase is absent in stacked membranes. It may reflect a non-equilibrium situation in stacked membranes, as expected if rapid PC diffusion and equilibration is restricted to domains. (However, relaxation kinetics are complex and the point certainly requires further analysis.) It is actually reasonable to believe that rapid transfer of plastocyanin from cyt *bf* in grana stacks is restricted to PSI centered around the grana in the grana margins (see discussion in [24,50]). This would then raise the question about the function of PSI located in distant stroma lamellae. There is still a number of unsolved questions concerning the microcompartmentation of electron transport processes in thylakoids.

Acknowledgements

The authors wish to thank Dr. E. Boekema for the communication of unpublished results, Dr. H.W. Trissl for help in analyzing the fluorescence induction curve from DCMU-poised thylakoids and M. in der Stroth and U. Mukherjee for correcting and preparing the manuscript.

Appendix. Model of electron transport

We assume that the electron fluxes through PSII and cyt *bf* complexes, v_{PSII} and v_{bf}, are given by the concentrations of enzyme–substrate complexes, (PSII-PQ) and (*bf*-PQH_2), multiplied with an apparent intrinsic constant for these complexes, k_{PSII} and k_{bf}.

$$v_{PSII} = k_{PSII}(PSII{-}PQ) \tag{A.1}$$

$$v_{bf} = k_{bf}(bf{-}PQH_2) \tag{A.2}$$

The concentrations of enzyme–substrate complexes are derived from dissociation constants of PQ and PQH_2 at the QB-site (PSII) and at the Q_o-site (cyt *bf* complex), in conjunction with the assumption that the overall concentrations of PSII ($PSII_o$), cyt *bf* complex (bf_o) and PQ (PQ_o) remain constant. The corresponding expressions are shown in the following equations (see illustration in Fig. 3):

$$K_D\mathrm{bf} = \frac{bf{\cdot}PQH_2}{(bf{-}PQH_2)} \tag{A.3}$$

$$K_D\mathrm{PSII} = \frac{PSII{\cdot}PQ}{(PSII{-}PQ)} \tag{A.4}$$

$$K_D bf_r = \frac{bf{\cdot}PQ}{(bf{-}PQ)} \tag{A.5}$$

$$K_D\mathrm{PSII}_r = \frac{PSII{\cdot}PQH_2}{(PSII{-}PQH_2)} \tag{A.6}$$

$$bf_o = bf + (bf{-}PQ) + (bf{-}PQH_2) \tag{A.7}$$

$$PSII_o = PSII + (PSII{-}PQ) + (PSII{-}PQH_2) \tag{A.8}$$

$$PQ_o = PQ + PQH_2 + (bf{-}PQ) + (bf{-}PQH_2) + (PSII{-}PQ) + (PSII{-}PQH_2) \tag{A.9}$$

From Eqs. A.1–A.9 and with the assumption ($v_{bf} = v_{PSII}$) for the steady state we derive an equation with ($bf{-}PQH_2$) as the only variable.

$$\frac{K_D\mathrm{PSII}_r[PSII_o - V(bf{-}PQH_2)]}{K_D\mathrm{PSII}_r + PQH_2} + Q_o - PQH_2 - bf_o - PSII_o + K_D bf_r = PQH_2\frac{bf_o - (bf{-}PQH_2)}{\frac{K_D bf}{K_D bf_r}(bf{-}PQH_2)} - \frac{K_D bf(bf{-}PQH_2)}{PQH_2} \tag{A.10a}$$

where

$$PQH_2 = \frac{(bf{-}PQH_2)^2 K_D bf{\cdot}V - (bf{-}PQH_2)^2 K_D\mathrm{PSII}_r{\cdot}V\frac{K_D\mathrm{PSII}}{K_D\mathrm{PSII}_r}\frac{K_D bf}{K_D bf_r} - (bf{-}PQH_2)K_D bf{\cdot}PSII_o}{(bf{-}PQH_2)V{\cdot}bf_o - (bf{-}PQH_2)^2 V + (bf{-}PQH_2)^2 V\frac{K_D\mathrm{PSII}}{K_D\mathrm{PSII}_r}\frac{K_D bf}{K_D bf_r} - bf_o{\cdot}PSII_o + (bf{-}PQH_2)PSII_o} \tag{A.10b}$$

The parameter V is the ratio of $k_{bf} \times bf_o / k_{PSII} \times PSII_o$. We assume that DCMU inhibited PSII-centers (1) do not contribute to linear electron transport and (2) do not bind to PQ or PQH_2. Inhibited centers reduce the number of active centers ($PSII_o$). The actual number of active PSII centers enters Eq. A.10a via the V term and directly by $PSII_o$.

We solve Eq. A.10a for ($bf{-}PQH_2$) yielding an equation of fifth order with respect to V. The zero points of this equation are calculated with Newton's approximation. The solution is selected by the condition that $0 < (bf{-}PQH_2) < bf_o$. This solution is inserted in Eq. A.2.

We assume that the electron transport rate given by Eq. A.2 determines the rate of steady state electron transport (see above). The dependency of the electron flux rate on the number of active PSII-centers is analyzed by varying $PSII_o$. The curves in Fig. 2B are calculated in this way for different parameter sets given in Table 6 and by normalizing Eq. A.2 to 1 if $PSII_o$ is maximal.

It is assumed in the model, that the intermediates PQ and PQH_2 can diffuse rapidly between all binding sites, i.e. no diffusion limitation exists.

Table 6
Parameters used for the electron transport model

	Literature	Curve 1	Curve 2
K_DPSII	1 to 2 mM[a]	1.5	1.5
K_DPSII$_r$	1 to 2 mM[a]	1.5	1.5
$K_D bf$	0.05 mM[b]	0.05	0.05
$K_D bf_r$	unknown	0.05	0.5
k_{PSII}/k_{bf}	see text, 1.7 to 2.5[c]	1.7	1.7
PQ (total)	1[b] to 14 mM[d]	1	7
PSII (total)		1/6 × PQ (total)[e]	
Cyt *bf* (total)		1/2 × PSII (total)[e]	

[a][48]
[b][72]
[c]We assume the smallest ratio for PSII to cyt *bf* turnover times, i.e. $(2\ ms)^{-1}$ for PSII $(3.3\ ms)^{-1}$ for cyt *bf*.
[d][18]
[e]Own measurements.

References

[1] B. Andersson, J.M. Anderson, Biochim. Biophys. Acta 593 (1980) 427–440.
[2] J.M. Anderson, FEBS Lett. 138 (1982) 62–66.
[3] J.M. Anderson, Photosynth. Res. 34 (1992) 341–357.
[4] L.A. Staehelin, in: L.A. Staehelin, C.J. Arntzen (Eds.), Photosynthesis III, Encyclopedia of Plant Physiology, vol. 19, Springer, Berlin, 1986, pp. 1–84.
[5] L.A. Staehelin, G.W.M. Van der Staay, in: D.A. Ort, C.F. Yocum (Eds.), Oxygenic Photosynthesis: the Light Reactions, Kluwer Academic Publishers, The Netherlands, 1996, pp. 11–30.
[6] H.H. Stiehl, H.T. Witt, Z. Naturforsch. 24b (1969) 1588–1598.
[7] W. Haehnel, Ann. Rev. Plant Physiol. 35 (1984) 659–693.
[8] M.F. Blackwell, K. Gounaris, S.J. Zara, J. Barber, Biophys. J. 51 (1987) 735–744.
[9] R. Mitchell, A. Spillmann, W. Haehnel, Biophys. J. 58 (1990) 1011–1024.
[10] L.A. Staehelin, C.J. Arntzen, J. Cell. Biol. 97 (1983) 1327–1337.
[11] J. Lavergne, J.-P. Bouchaud, P. Joliot, Biochim. Biophys. Acta 1101 (1992) 13–22.
[12] D.J. Murphy, Biochim. Biophys. Acta 864 (1986) 33–94.
[13] M.F. Blackwell, J. Whitmarsh, Biophys. J. 58 (1990) 1259–1271.
[14] M.J. Saxton, Biophys. J. 56 (1989) 615–622.
[15] M.J. Saxton, Biophys. J. 61 (1992) 119–128.
[16] W.Y. Shih, I.A. Aksay, R. Kikuchi, Phys. Rev. 36 (1987) 5015–5019.
[17] P.A. Millner, D.J. Chapman, J. Barber, Biochim. Biophys. Acta 765 (1984) 282–287.
[18] M. Blackwell, C. Gibas, S. Gygax, D. Roman, B. Wagner, Biochim. Biophys. Acta 1183 (1994) 533–543.
[19] J. Lavergne, P. Joliot, Trends Biochem. Sci. 16 (1991) 129–134.
[20] P. Joliot, J. Lavergne, D. Béal, Biochim. Biophys. Acta 1101 (1992) 1–12.
[21] P. Joliot, A. Joliot, Biochim. Biophys. Acta 1102 (1992) 53–61.
[22] J. Lavergne, P. Joliot, Photosynth. Res. 48 (1996) 127–138.
[23] J.M. Anderson, W.W. Thomson, in: W.R. Briggs (Ed.), Photosynthsis, Alan Liss, New York, 1989, pp. 161–182.
[24] P.-A. Albertsson, Photosynth. Res. 46 (1995) 141–149.
[25] M. Rögner, E.J. Boekema, J. Barber, Trends Biochem. Sci. 21 (1996) 44–49.
[26] R. Bassi, P. Dianese, Eur. J. Biochim. 204 (1992) 317–326.
[27] B. Hankamer, J. Barber, E.J. Boekema, Annu. Rev. Plant Physiol. Plant Mol. Biol. 48 (1997) 641–671.
[28] E.J. Boekema, H. van Roon, F. Calkoen, R. Bassi, J.P. Dekker, Biochemistry 38 (1999) 2233–2239.
[29] J.P. Dekker, H. van Roon, E.J. Boekema, FEBS Lett. 449 (1999) 211–214.
[30] J. Barber, Biochim. Biophys. Acta 594 (1980) 253–308.
[31] J.F. Allen, Biochim. Biophys. Acta 1098 (1992) 275–335.
[32] R. Bassi, D. Sandona, R. Croce, Physiol. Plant. 100 (1997) 769–779.
[33] H. Laasch, Planta 171 (1987) 220–226.
[34] H.W. Trissl, J. Lavergne, Aust. J. Plant Physiol. 22 (1994) 183–193.
[35] R. Reich, R. Scheerer, K.-U. Sewe, H.T. Witt, Biochim. Biophys. Acta 449 (1976) 285–294.
[36] P. Joliot, A. Joliot, Biochim. Biophys. Acta 765 (1984) 210–218.
[37] J. Barber, in: M.D. Hatch, N.K. Boardman (Eds.), The Biochemistry of Plants, vol. 10, 1987, pp. 75–130.
[38] G.H. Krause, E. Weis, Annu. Rev. Plant Physiol. Plant Physiol. Mol. Biol. 42 (1991) 313–349.
[39] S. Murakami, L. Packer, Arch. Biochim. Biophys. 146 (1971) 337–347.
[40] H. Kacser, J.A. Burns, Biochem. Soc. Trans. Biochem Soc. 7 (1979) 1149–1160.
[41] W.A. Cramer, G.M. Soriano, M. Ponomarev, D. Huang, H.

Zhang, S.E. Martinez, J.L. Smith, Annu. Rev. Plant Physiol. Plant Mol. Biol. 47 (1996) 477–508.
[42] G. Hauska, M. Schütz, M. Büttner, in: D.A. Ort, C.F. Yocum (Eds.), Oxygenic Photosynthesis: the Light Reactions, Kluwer Academic Publishers, The Netherlands, 1996, pp. 377–398.
[43] D.A. Ort, J. Whitmarsh, Photosynth. Res. 23 (1990) 101–104.
[44] Govindjee, Photosynth. Res. 25 (1990) 151–160.
[45] A.W. Rutherford, Trends Biochem. Sci. 14 (1989) 227–232.
[46] Ö. Hansson, T. Wydrzynski, Photosynt. Res. 23 (1990) 131–162.
[47] W. Ausländer, W. Junge, Biochim. Biophys. Acta 357 (1974) 285–298.
[48] A.B. Diner, V. Petrouleas, J.J. Wendoloski, Physiol. Plant. 81 (1991) 423–436.
[49] J.M. Anderson, W.S. Chow, D.J. Goodchild, Aust. J. Plant Physiol. 15 (1988) 11–26.
[50] A.B. Hope, Biochim. Biophys. Acta 1143 (1993) 1–22.
[51] T. Kallas, in: D.A. Bryant (Ed.), The Molecular Biology of Cyanobacteria, Kluwer Academic Publishers, The Netherlands, 1994, pp. 185–219.
[52] S. Malkin, B. Kok, Biochim. Biophys. Acta 126 (1966) 413–432.
[53] D.A. Fell, Biochem. J. 286 (1992) 313–330.
[54] W. Kühlbrandt, D.N. Wang, Y. Fujiyoshi, Nature 367 (1994) 614–621.
[55] P.J. Morissey, R.R. Glick, A. Melis, Plant Cell Physiol. 30 (1989) 335–344.
[56] R. Van Grondelle, J. Amesz, in: Govindjee, J. Amesz, D.C. Fork (Eds.), Light Emission by Plant and Bacteria, Academic Press, New York, 1986, pp. 191–223.
[57] W.L. Butler, Annu. Rev. Plant. Physiol. 29 (1978) 345–378.
[58] J. Bennet, Annu. Rev. Plant Physiol. Plant Mol. Biol. 42 (1991) 281–311.
[59] O. Vallon, F.A. Wollman, J. Olive, Photochem. Photobiophys. 12 (1986) 203–220.
[60] F. Drepper, I. Carlberg, B. Andersson, W. Haehnel, Biochemistry 32 (1993) 11915–11922.
[61] P. Joliot, A. Verméglio, A. Joliot, Biochim. Biophys. Acta 1141 (1993) 151–174.
[62] J.M. Anderson, W.S. Chow, Y.-I. Park, Photosynth. Res. 46 (1995) 129–139.
[63] H.W. Trissl, C. Wilhelm, Trends Biochem. Sci. 18 (1993) 415–419.
[64] E.L. Gross, in: D.A. Ort, C.F. Yocum (Eds.), Oxygenic Photosynthesis, Kluwer Academic Publishers, The Netherlands, 1996, pp. 413–429.
[65] W. Haehnel, R. Ratajczak, H. Robenek, J. Cell. Biol. 108 (1989) 1397–1405.
[66] R. Delosme, Photosynth. Res. 29 (1991) 45–54.
[67] S.U. Metzger, W.A. Cramer, J. Whitmarsh, Biochim. Biophys. Acta 1319 (1997) 233–241.
[68] N. Nelson, J. Neumann, J. Biol. Chem. 247 (1972) 1817–1824.
[69] H.J. Van Gorkum, Biochim. Biophys. Acta 347 (1974) 439–442.
[70] B. Ke, Arch. Biochim. Biophys. 152 (1972) 70–77.
[71] S. Katoh, I. Suga, I. Shiratori, A. Takamiya, Arch. Biochim. Biophys. 94 (1961) 136–141.
[72] D.M. Kramer, A. Joliot, P. Joliot, A.R. Crofts, Biochim. Biophys. Acta 1184 (1994) 251–262.
[73] D. Bald, J. Kruip, E.J. Boekema, M. Rögner, in: N. Murata (Ed.), Research of Photosynthesis, vol. 1, Kluwer Academic Publishers, The Netherlands, 1992, pp. 629–632.
[74] B. Kok, P. Joliot, M.P. McCloin, Prog. Photosynth. Res. 11 (1969) 1042–1056.